Supporting Information for

Theoretical study for the evolution with chemical forms of fission products Cs and I elements in HTR-10

Kerong Wang, Jingni Guo, Feng Xie, Peng Li*, and Jie Ma

harmonic frequencies.

Table S4. Comparison of observed values and calculated bond lengths for CsOH.

Table S5. Comparison of observed values and calculated harmonic frequencies for CsOH.

Table S6. Comparison of observed values of IO with calculated bond lengths and calculated harmonic frequencies.

Table S7. Comparison of observed values and calculated bond lengths for IOH.

Table S8. Comparison of observed values and calculated harmonic frequencies for IOH.

Table S9. Topological properties of the charge density calculated in the reaction of $Cs+H_2O$.

Table S10. Reaction rate constants for $I/Cs+H_2O$ at 500-1000K.

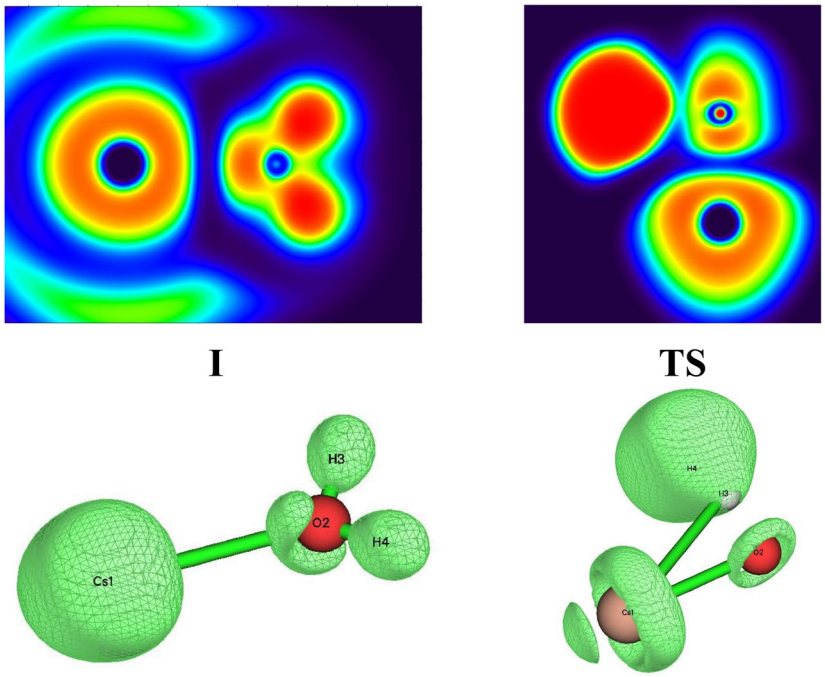

Figure S1. ELF shadow plane projection and three-dimensional isosurface diagram of each stagnation point in Cs and H_2O reaction process calculated by B3PW91/ def2-QZVPPD/aug-cc-pVTZ theory.

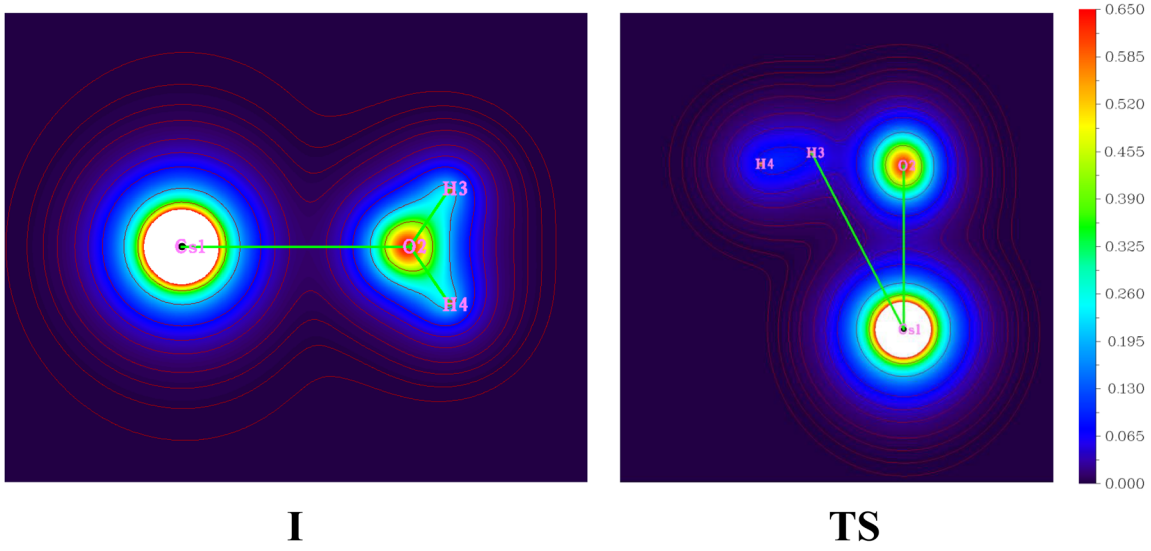

Figure S2. Color-filled map of BOD for Cs+H_2O.

I

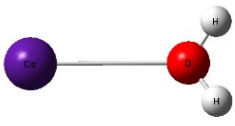

	x	y	z
Cs	0.48123600	0.00000000	-0.00124200
O	-2.54129000	-0.00001000	0.05746700
H	-3.06875900	0.76726800	-0.19569200
H	-3.06891600	-0.76716800	-0.19572300

TS

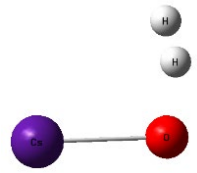

	x	y	z
Cs	0.39942000	0.00790100	0.00000000
O	-2.11649600	-0.40081200	0.00000000
H	-2.54255300	0.98093700	0.00000000
H	-2.49359800	1.79100000	0.00000000

Figure S3. Optimized Cartesian x, y, z coordinates for the reaction of Cs+H_2O at the B3PW91/ def2-QZVPPD /aug-cc-pVTZ level of theory.

I

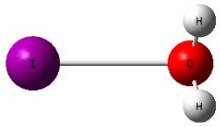

	x	y	z
I	-0.45369400	0.00000000	0.00096400
O	2.37197800	0.00000000	-0.11715500
H	2.53498300	-0.76413600	0.44305900
H	2.53498400	0.76413600	0.44306000

TS1

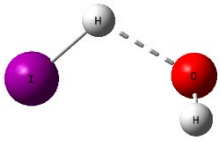

	x	y	z
I	-0.43197000	-0.01154300	-0.00409500
O	2.45546900	0.04089800	-0.08203200
H	2.49275700	-0.73975100	0.49329500
H	0.75788700	1.02436200	0.37999300

II

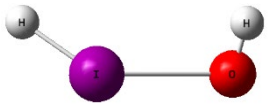

	x	y	z
I	0.33826100	-0.02837500	-0.01042200
O	-2.13757700	-0.03117100	0.09089700
H	-2.32410200	0.69322000	-0.52418200
H	1.49689300	1.06004100	0.34938900

TS2

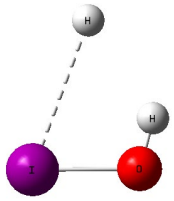

	x	y	z
I	-0.30756400	-0.00995100	0.00000000
O	1.63977600	-0.32214700	-0.00000100
H	2.03244800	0.55859300	-0.00000100
H	1.15024200	2.54596800	0.00000100

III

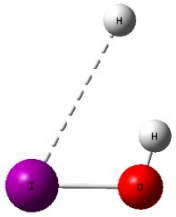

	x	y	z
I	0.06285400	-0.31060500	0.00000000
O	0.06285400	1.66285300	0.00000000
H	-0.86748500	1.91470400	0.00000000
H	-2.96661100	1.24452800	0.00000000

TS3

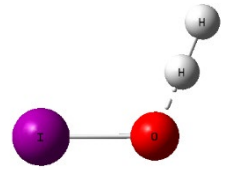

	x	y	z
I	0.04866400	-0.32681100	0.00000000
O	0.04866400	1.61023900	0.00000000
H	-1.05341900	2.05309100	0.00000000
H	-1.91508000	2.38596300	0.00000000

TS4

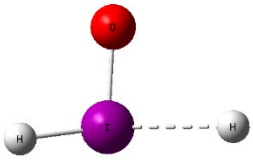

	x	y	z
I	0.22954400	-0.00014500	-0.01821300
O	-1.59261600	-0.08359900	0.00734000
H	0.62427400	-1.52954400	0.53409600
H	-0.04918800	2.20603500	0.37247500

IV

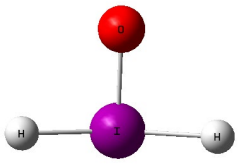

	x	y	z
I	0.23182100	0.00000000	-0.01792900
O	-1.58938700	0.00000100	-0.00115400
H	0.21429300	-1.70358000	0.47975000
H	0.21429900	1.70359900	0.47974500

TS2'

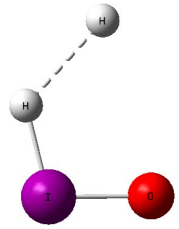

	x	y	z
I	-0.24967300	-0.04650800	0.00000100
O	1.56651200	-0.25812700	-0.00000500
H	-0.43015400	1.60337500	0.00000000
H	1.13073100	2.92655100	-0.00000600

TS5

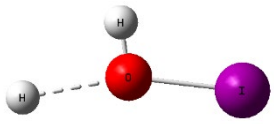

	x	y	z
I	0.35125600	-0.00737500	0.00000200
O	-1.65671700	0.00166500	-0.00004000
H	-1.89681700	0.93554800	0.00007600
H	-3.46603000	-0.55796900	0.00012500

TS6

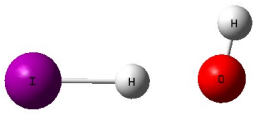

	x	y	z
I	0.49203000	0.00202400	0.00000000
O	-2.73447100	-0.10677400	0.00000100
H	-2.99918100	0.82951500	0.00000700
H	-1.20262700	-0.08258900	-0.00000200

Figure S4. Optimized Cartesian x, y, z coordinates for the reaction of I+H_2O at the PBE0/LANL2DZdp/aug-cc-pVTZ level of theory.

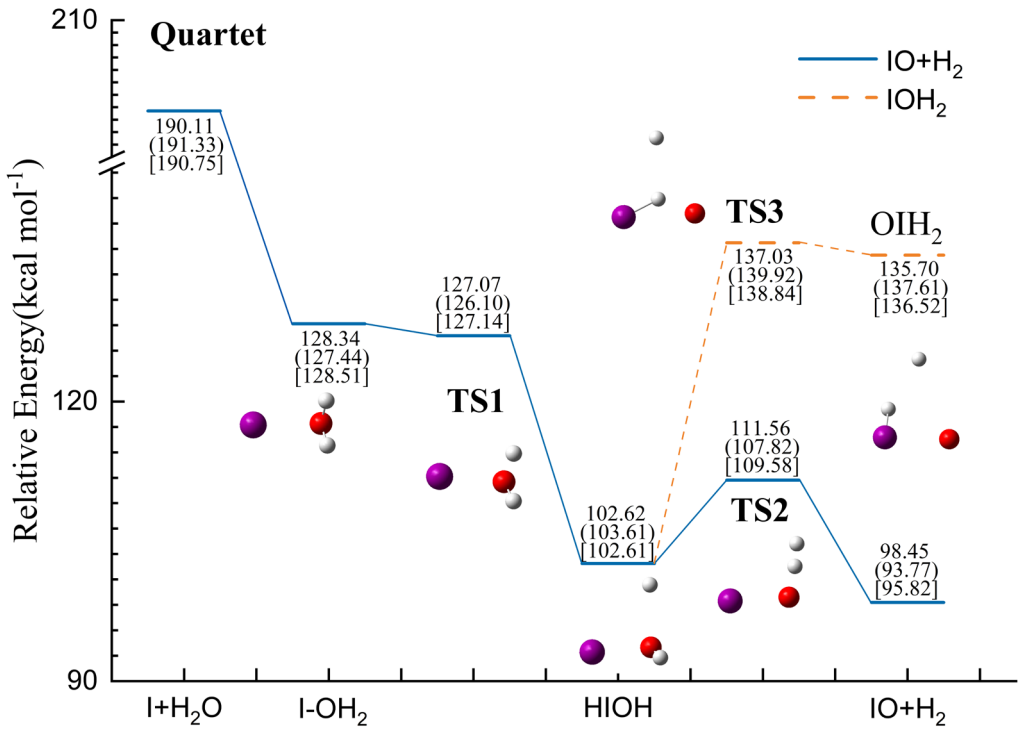

Figure S5. Potential energy profile for the reaction of I + H_2O computed at the PBE0/LANL2DZdp/aug-cc-pVTZ levels of theory. B3LYP and B3PW91 energy parameters are reported in ( ) and [ ] respectively.

For the reaction of I atom with H_2O in the quartet state, there is a division into isomerization and dehydrogenation channels. The PES curves for I+H_2O are shown in Figure S5. It can be seen that the reaction process is similar to that of the doublet state. Firstly, the I atom combines with the H_2O molecule to the reactant complex I-OH_2(I). This process releases energy 61.77 kcal mol^{-1}. Then, the H-O bond is broken to give the first transition state. It has an imaginary frequency of 1724.5 cm^{-1}, which corresponds to the process of H atom moving away. It is noteworthy that the Gibbs free energy of I-OH_2 is slightly higher than that of TS1. But comparing their electron energies leads to the opposite conclusion. This is a common and normal phenomenon.[1-2] After crossing the first transition state, the intermediate HIOH is formed. From then on, there is a division into isomerization and dehydrogenation channels. The isomerization product H_2IO is formed via TS3.The activation barrier to be overcome for the formation of TS3 is 34.41 kcal mol^{-1}. It has an imaginary frequency of 408.4 cm^{-1}, corresponds to the vibrational mode of H transfer from O atom to I atom. The dehydrogenation channel undergoes the transition state of TS2. The activation barrier to be overcome for its formation is 8.9 kcal mol^{-1}. It has an imaginary frequency of 1321.6 cm^{-1}, corresponds to a vibrational mode in which the two H atoms move away from the main frame IO. Finally, this reaction forms the product

monomers IO + H_2.

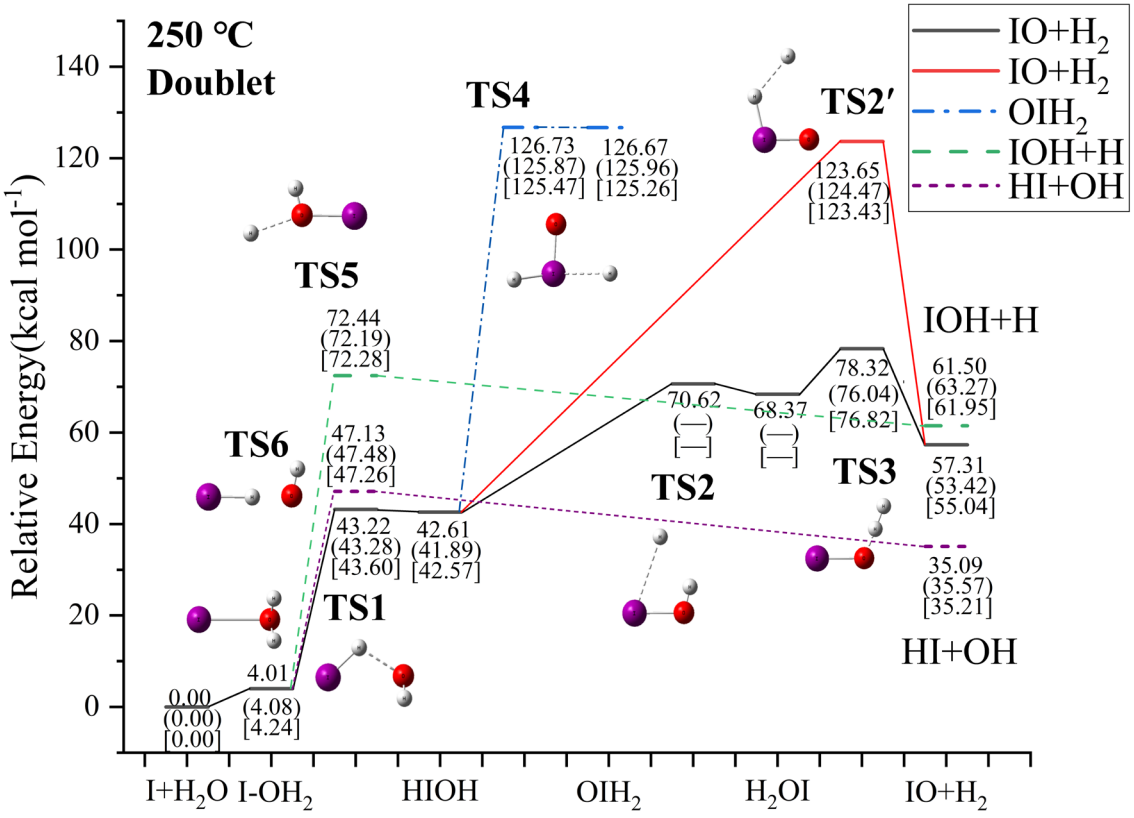

Figure S6. Potential energy profile for the reaction of I + H_2O at 250 °C computed on the PBE0/LANL2DZdp/aug-cc-pVTZ levels of theory. B3LYP and B3PW91 energy parameters are reported in ( ) and [ ] respectively.

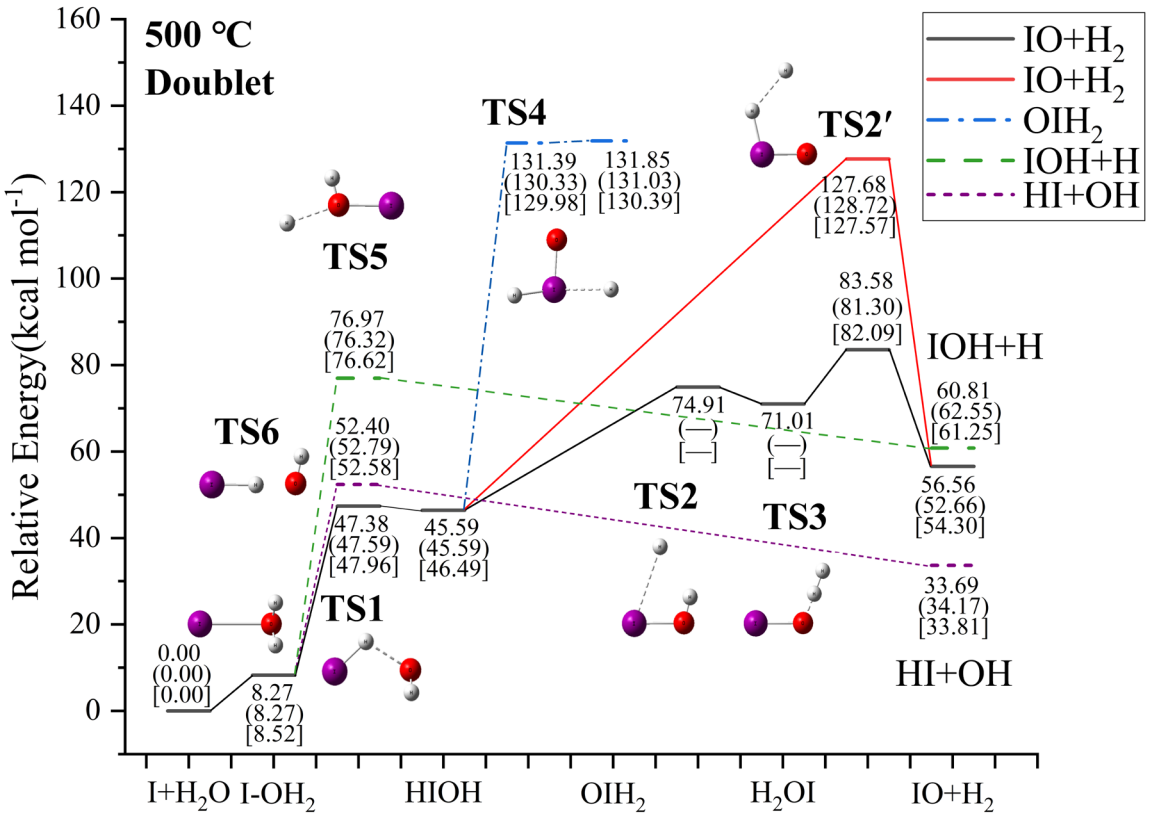

Figure S7. Potential energy profile for the reaction of I + H_2O at 500 °C computed on the PBE0/LANL2DZdp/aug-cc-pVTZ levels of theory. B3LYP and B3PW91 energy parameters are reported in ( ) and [ ] respectively.

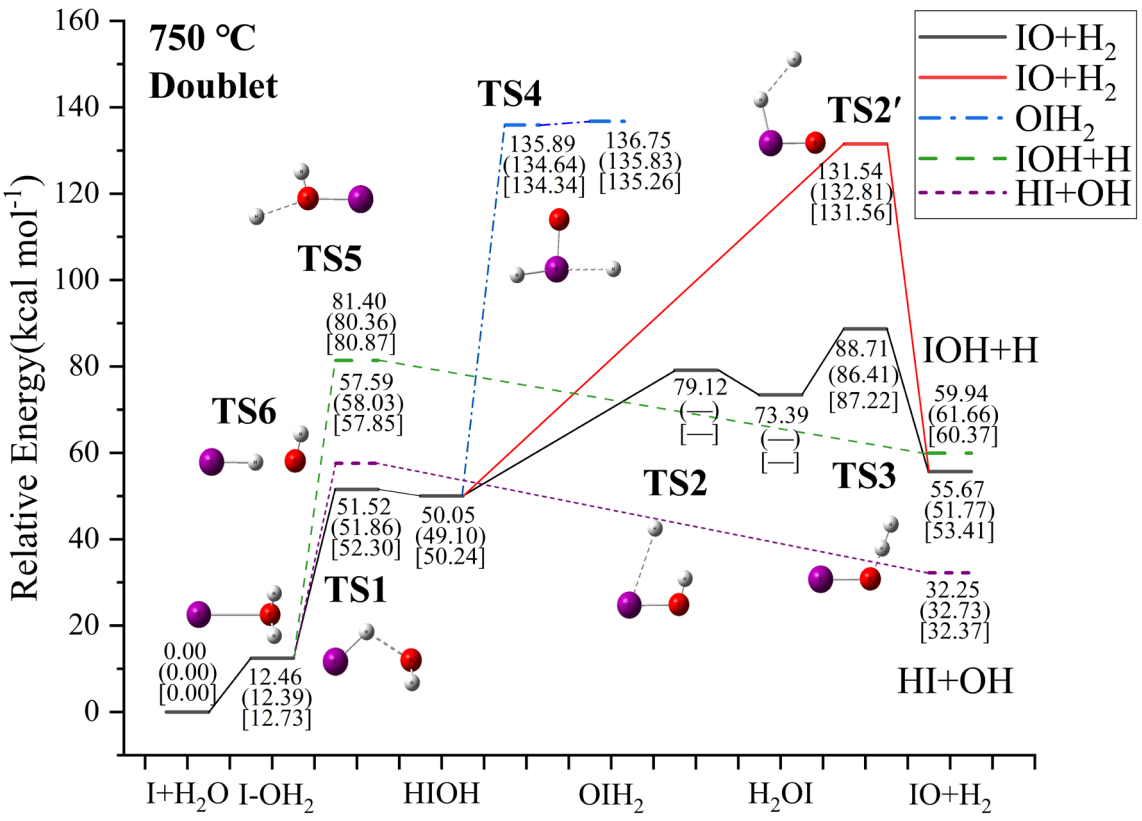

Figure S8. Potential energy profile for the reaction of I + H_2O at 750 °C computed on the PBE0/LANL2DZdp/aug-cc-pVTZ levels of theory. B3LYP and B3PW91 energy parameters are reported in ( ) and [ ] respectively.

Table S1. Raw and BSSE corrected energies of the complexes of I+H_2O and their difference.

Species	Energy(raw)	Energy(corrected)	**ΔE**(BSSE)/Hartree	**ΔE**(BSSE)/Kcal mol^{-1}
I	-87.7527	-87.7523	0.00043	0.269829
TS1	-87.6822	-87.682	0.000197	0.123619
II	-87.6842	-87.684	0.000242	0.151857
TS2	-87.6369	-87.6368	0.00013	0.081576
III	-87.637	-87.6362	0.000768	0.481927
TS3	-87.6236	-87.6228	0.000777	0.487575
TS2'	-87.5471	-87.5469	0.000197	0.123619
TS4	-87.5443	-87.544	0.000349	0.219001
IV	-87.5488	-87.5474	0.001471	0.923067
TS5	-87.6348	-87.6344	0.000332	0.208333
TS6	-87.6776704	-87.677164	0.000506	0.317771

Table S2. Raw and BSSE corrected energies of the complexes of Cs+H_2O and their difference.

Species	Energy(raw)	Energy(corrected)	**ΔE**(BSSE)/Hartree	**ΔE**(BSSE)/Kcal mol^{-1}
I	-96.6196	-96.6196	3E-05	0.018825
TS	-96.5313	-96.5312	0.000139	0.087224

Table S3. Comparison of observed values of CsO with calculated bond lengths and calculated harmonic frequencies. [a] Calculations used the def2-QZVPPD for Cs and 6-311++G** for H and O atoms. [b] Calculations used the def2-QZVPPD for Cs and aug-cc-pVTZ for H and O atoms.

Method	r(Cs-O)	Frequencies(cm^{-1})
B3LYP[a]	2.364	342.5
B3LYP[b]	2.350	346.1
B3LYP-D3[b]	2.349	346.2
PBE0[a]	2.329	353.2
PBE0[b]	2.311	357.9
PBE0-D3[b]	2.311	357.9
PBE [a]	2.319	344.6
PBE [b]	2.302	348.9
PBE-D3 [b]	2.302	348.9
PW91[b]	2.302	349.9
B3PW91[a]	2.333	350.5
B3PW91[b]	2.317	354.9
B3PW91-D3[b]	2.317	355.0
Expt	2.300	357.0

Table S4. Comparison of observed values and calculated bond lengths for CsOH. [a] Calculations used the def2-QZVPPD for Cs and 6-311++G** for H and O atoms. [b] Calculations used the def2-QZVPPD for Cs and aug-cc-pVTZ for H and O atoms.

Method	r(O-H)	r(Cs-O)
B3LYP[a]	0.960	2.433
B3LYP[b]	0.959	2.428
B3LYP-D3[b]	0.959	2.427
PBE0[a]	0.957	2.405
PBE0[b]	0.957	2.398
PBE0-D3[b]	0.957	2.400
PBE [a]	0.968	2.413
PBE [b]	0.968	2.409
PBE-D3 [b]	0.968	2.409
PW91[b]	0.967	2.408
B3PW91[a]	0.958	2.411
B3PW91[b]	0.958	2.405
B3PW91-D3[b]	0.957	2.404
Expt	0.920	2.403

Table S5. Comparison of observed values and calculated harmonic frequencies for CsOH. [a] Calculations used the def2-QZVPPD for Cs and 6-311++G** for H and O atoms. [b] Calculations used the def2-QZVPPD for Cs and aug-cc-pVTZ for H and O atoms.

Method	Frequencies(cm^{-1})			
B3LYP[a]	356.2	356.2	367.6	3885.0
B3LYP[b]	323.3	323.3	367.1	3857.6
B3LYP-D3[b]	321.8	321.8	367.9	3859.0
PBE0[a]	361.4	361.4	379.0	3944.9
PBE0[b]	324.2	324.2	378.5	3916.5
PBE0-D3[b]	323.8	323.8	378.7	3916.9

PBE[a]	321.9	321.9	371.8	3785.2
PBE [b]	295.5	295.5	369.7	3751.3
PBE-D3 [b]	294.9	294.9	370.0	3751.8
PW91[b]	296.4	296.4	370.8	3757.0
B3PW91[a]	355.8	355.8	375.4	3915.7
B3PW91[b]	319.8	319.8	375.0	3887.4
B3PW91-D3[b]	309.3	309.3	375.6	3893.7
Expt	306.0	306.0	336.0	3705.0

Table S6. Comparison of observed values of IO with calculated bond lengths and calculated harmonic frequencies. Calculations used the LANL2DZdp for I and aug-cc-pVTZ for H and O atoms.

Method	r(I-O)	Frequencies(cm^{-1})
B3LYP	1.869	667.9
B3LYP-D3	1.869	668.0
PBE0	1.863	681.4
PBE0-D3	1.863	681.5
B3PW91	1.865	679.4
B3PW91-D3	1.865	679.5
Expt	1.868	681.6

Table S7. Comparison of observed values and calculated bond lengths for IOH. Calculations used the LANL2DZdp for I and aug-cc-pVTZ for H and O atoms.

Method	r(I-O)	r(H-O)
B3LYP[a]	1.987	0.965
B3LYP-D3[a]	1.988	0.965
PBE0[a]	1.975	0.962
PBE0-D3[a]	1.975	0.962
B3PW91[a]	1.981	0.964
B3PW91-D3[a]	1.981	0.964
Expt	1.959–1.995	0.960

Table S8. Comparison of observed values and calculated harmonic frequencies for IOH. Calculations used the LANL2DZdp for I and aug-cc-pVTZ for H and O atoms.

Method	Frequencies(cm^{-1})		
B3LYP[a]	573.8	1101.1	3795.0
B3LYP-D3[a]	573.2	1101.3	3795.8
PBE0[a]	598.7	1108.3	3851.7
PBE0-D3[a]	598.6	1108.6	3851.6
B3PW91[a]	587.1	1103.3	3822.4
B3PW91-D3[a]	587.7	1103.9	3822.9
Expt	575.0	1068.0	3625.8

Table S9. Topological properties of the charge density calculated at the (3,-1) BCP for all species involved in the reaction of Cs+H_2O at the B3PW91/def2-QZVPPD/aug-cc-pVTZ level of theory.

	Species	$\rho(r)$	$\nabla^2\rho(r)$	G(r)	V(r)	H(r)	η
I	Cs-O	0.015	0.060	0.012	−0.010	−0.013	1.865
	O-H	0.365	−2.638	0.076	−0.812	−0.077	1.865

	O-H	0.365	−2.638	0.076	−0.812	−0.077	0.155
TS1	Cs-O	0.047	0.152	0.040	−0.044	−0.041	0.201
	O-H	0.087	0.121	0.065	−0.101	−0.066	0.370
	H-H	0.219	−0.839	0.010	−0.230	−0.010	1.254
CsO	CsO	0.063	0.234	0.067	−0.077	−0.067	0.161

Table S10. Reaction rate constants for I/Cs+H_2O at 500-1050K.

T, K	I-OH_2 → TS1 → HIOH			HIOH → TS2 → H_2OI			H_2OI → TS3 → IO+H_2		
	K^{VTST}	$K^{VTST/W}$	$K^{VTST/Eck}$	K^{VTST}	$K^{VTST/W}$	$K^{VTST/Eck}$	K^{VTST}	$K^{VTST/W}$	$K^{VTST/Eck}$
500	8.56×10^{-5}	8.66×10^{-5}	8.48×10^{-5}	3.24	3.42	2.38	4.11×10^{3}	4.34×10^{3}	4.36×10^{3}
550	0.00	0.00	0.00	41.06	42.98	30.62	1.88×10^{4}	1.97×10^{4}	1.98×10^{4}
600	0.08	0.08	0.08	3.42×10^{2}	3.56×10^{2}	2.59×10^{2}	6.64×10^{4}	6.90×10^{4}	6.92×10^{4}
650	1.06	1.07	1.04	2.06×10^{3}	2.13×10^{3}	1.58×10^{3}	1.93×10^{5}	1.99×10^{5}	2.00×10^{5}
700	10.07	10.13	9.67	9.64×10^{3}	9.64×10^{3}	7.36×10^{3}	4.79×10^{5}	4.93×10^{5}	4.94×10^{5}
750	71.18	71.55	68.24	3.68×10^{4}	3.77×10^{4}	2.84×10^{4}	1.05×10^{6}	1.08×10^{6}	1.08×10^{6}
800	3.95×10^{2}	3.97×10^{2}	3.79×10^{2}	1.19×10^{5}	1.22×10^{5}	9.25×10^{4}	2.09×10^{6}	2.14×10^{6}	2.15×10^{6}
850	1.80×10^{3}	1.81×10^{3}	1.73×10^{3}	3.35×10^{5}	3.42×10^{5}	2.63×10^{5}	3.84×10^{6}	3.91×10^{6}	3.92×10^{6}
900	6.93×10^{3}	6.96×10^{3}	6.68×10^{3}	8.44×10^{5}	8.59×10^{5}	6.67×10^{5}	6.57×10^{6}	6.69×10^{6}	6.72×10^{6}
950	2.32×10^{4}	2.33×10^{4}	2.28×10^{4}	1.93×10^{6}	1.96×10^{6}	1.56×10^{6}	1.06×10^{7}	1.08×10^{7}	1.08×10^{7}
1000	6.91×10^{4}	6.93×10^{4}	6.88×10^{4}	4.07×10^{6}	4.13×10^{6}	3.30×10^{6}	1.64×10^{7}	1.66×10^{7}	1.67×10^{7}

T, K	HIOH → TS4 → OIH_2			I-OH_2 → TS5 → IOH+H		
	K^{VTST}	$K^{VTST/W}$	$K^{VTST/Eck}$	K^{VTST}	$K^{VTST/W}$	$K^{VTST/Eck}$
500	1.11×10^{-24}	1.22×10^{-24}	1.14×10^{-24}	9.76×10^{-17}	9.84×10^{-17}	9.79×10^{-17}
550	2.20×10^{-21}	2.39×10^{-21}	2.24×10^{-21}	5.28×10^{-14}	5.32×10^{-14}	5.29×10^{-14}
600	1.23×10^{-18}	1.32×10^{-18}	1.25×10^{-18}	1.01×10^{-11}	1.02×10^{-11}	1.01×10^{-11}
650	2.63×10^{-16}	2.79×10^{-16}	2.65×10^{-16}	8.68×10^{-10}	8.68×10^{-10}	8.61×10^{-10}
700	2.62×10^{-14}	2.76×10^{-14}	2.57×10^{-14}	3.97×10^{-8}	3.97×10^{-8}	3.86×10^{-8}
750	1.42×10^{-12}	1.48×10^{-12}	1.39×10^{-12}	1.10×10^{-6}	1.10×10^{-6}	1.06×10^{-6}
800	4.67×10^{-11}	4.86×10^{-11}	4.57×10^{-11}	2.01×10^{-5}	2.02×10^{-5}	1.94×10^{-5}
850	1.02×10^{-9}	1.06×10^{-9}	9.99×10^{-10}	2.63×10^{-4}	2.64×10^{-4}	2.52×10^{-4}
900	1.60×10^{-8}	1.65×10^{-8}	1.56×10^{-8}	0.00	0.00	0.00
950	1.87×10^{-7}	1.92×10^{-7}	1.85×10^{-7}	0.02	0.02	0.02
1000	1.72×10^{-6}	1.76×10^{-6}	1.70×10^{-6}	0.13	0.13	0.12

T, K	I-OH_2 → TS6 → HI+OH			Cs-OH_2 → TS → CsO+H_2O		
	K^{VTST}	$K^{VTST/W}$	$K^{VTST/Eck}$	K^{VTST}	$K^{VTST/W}$	$K^{VTST/Eck}$
500	1.10×10^{-6}	1.11×10^{-6}	1.06×10^{-6}	1.71×10^{-9}	1.86×10^{-9}	1.79×10^{-9}
550	5.46×10^{-5}	5.52×10^{-5}	5.28×10^{-5}	1.58×10^{-7}	1.69×10^{-7}	1.63×10^{-7}
600	0.00	0.00	0.00	6.90×10^{-6}	7.33×10^{-6}	7.08×10^{-6}
650	0.02	0.02	0.02	1.70×10^{-4}	1.79×10^{-4}	1.74×10^{-4}
700	0.24	0.24	0.23	0.00	0.00	0.00
750	1.90	1.91	1.82	0.03	0.03	0.03
800	11.57	11.63	11.01	0.24	0.25	0.24
850	57.13	57.39	54.74	1.54	1.58	1.51
900	2.37×10^{2}	2.38×10^{2}	2.27×10^{2}	8.05	8.27	7.89
950	8.47×10^{2}	8.50×10^{2}	8.22×10^{2}	35.54	36.41	35.59
1000	2.67×10^{3}	2.68×10^{3}	2.59×10^{3}	1.36×10^{2}	1.39×10^{2}	1.36×10^{2}

[1] Z Zhao, Y.-X.; Wu, X.-N.; Ma, J.-B.; He, S.-G.; Ding, X.-L. Experimental and Theoretical Study of the Reactions between Vanadium-SiliconHeteronuclear Oxide Cluster Anions with N-Butane, J. Phys. Chem. C 2010,114, 12271-12279.

[2] Feyel, S.; Döbler, J.; Hoeckendorf, R.; Beyer, M. K.; Sauer,J.; Schwarz, H. Activation of Methane by Oligomeric [(Al2o3)X+ (X=3,4,5)]: TheRole of Oxygen-Centered Radicals in Thermal Hydrogen-Atom Abstraction, Angew. Chem. Int. Ed. 2008,47, 1946-1950.